A numerical study of coupled consolidation in unsaturated soils

Tai T. Wong, Delwyn G. Fredlund, and John Krahn

Abstract: This paper first describes the numerical implementation of the coupled formulation for the theory of consolidation of unsaturated soils. The developed computer code is verified using the Mandel–Cryer problem and then is applied to the solution of coupled multidimensional consolidation problems. Using a parametric study, it is demonstrated that, in unsaturated soils, the Mandel–Cryer effect is suppressed and the consolidation process in unsaturated soils is affected significantly by the shape of the soil-water characteristic curve. Finally, the developed model is used to analyze the consolidation of an unsaturated–saturated soil column. Analysis results indicate that the classical "undrained" pore-water pressure response to an externally applied load only occurs in the saturated zone while the pore-water pressure response is subdued in the unsaturated zone. This paper also shows a method of deriving one of the two additional material parameters required for the analysis of unsaturated soils from laboratory test results.

Key words: coupled consolidation, unsaturated soils, Mandel–Cryer effect, soil-water characteristic curve.

Résumé : Cet article décrit d'abord l'implémentation de la formulation couplée de la théorie de la consolidation des sols non saturés. Le code de calcul développé est vérifié sur le problème de Mandel–Cryer puis il est appliqué à la solution de problèmes couplés de consolidation multidimensionnelle. A partir d'une étude paramétrique, on a pu démontrer que l'effet de Mandel–Cryer disparaît dans les sols non saturés et que le processus de consolidation de ces matériaux est sensiblement affecté par la forme de la courbe caractéristique sol eau. Finalement on utilise le modèle développé pour analyser la consolidation d'une colonne de sol non saturé – saturé. Les résultats de l'analyse indiquent que la réponse classique «non drainée» de l'eau interstitielle à une charge appliquée extérieure n'intervient que dans la zone saturée, alors que cette réponse est faible dans la zone non saturée. Cet article donne également une méthode qui permet de déterminer, à partir des résultats d'essais de laboratoire, deux paramètres physiques supplémentaires nécessaires à l'analyse des sols non saturés.

Mots clés : consolidation couplée, sols non saturés, effet Mandel–Cryer, courbe caractéristique sol eau.

[Traduit par la Rédaction]

Introduction

There is a wide variety of practical problems where it is important to include both the unsaturated and the saturated consolidation in an analysis. A common situation is the placement of fill on the ground surface where the water table is at some depth. The transient conditions at the water table due to the applied load make it necessary to include both the saturated and the unsaturated consolidation. An example at the end of this paper is used to illustrate this case. Another common case is the pore-water pressure buildup in earth fill during construction, for example, in the core of an earth dam. The fill is placed in an unsaturated condition with the pore-water pressure at some negative state. As additional fill is being placed, the pore-water pressure in the fill will rise (become less negative) and eventually can be positive if the fill height becomes high enough. At near surface, the shrinking and swelling of soils due to environmental changes are also a form of consolidation. The soil changes volume in response to an applied loading arising from a change in negative pore-water pressure (or suction). The process is similar to consolidation. An unsaturated–saturated analysis is consequently required to correctly model such volume-change behaviour. Although the formulation of this paper is discussed in terms of consolidation, the concepts presented can be applied equally to the volume change associated with swelling and shrinking.

The formulation and description of coupled and uncoupled theories of consolidation for saturated soils can be traced back to the inception of classical soil mechanics. The subsequent solution of the coupled theory of consolidation led to an understanding of the Mandel–Cryer effect and the differences in pore-water pressures computed from coupled and uncoupled solutions to the consolidation problem. The Mandel–Cryer effect is the phenomenon in which the induced pore-water pressure may become higher than the applied pressure in a saturated soil. It was first described by Mandel (1953) for a triaxial soil sample and by Cryer (1963) for a spherical soil sample. In order to capture this effect mathematically, a three-dimensional consolidation theory is required (Schiffman et al. 1969).

Fully coupled formulations for the theory of consolidation (and the theory of swelling) for unsaturated soils were

Received December 5, 1997. Accepted July 15, 1998.

T.T. Wong. O'Connor Associates, Suite 1000, 639–5th Avenue SW, Calgary, AB T2P 0M9, Canada.
D.G. Fredlund. Department of Civil Engineering, University of Saskatchewan, 57 Campus Drive, Saskatoon, SK S7N 5A9, Canada.
J. Krahn. GEO-SLOPE International Ltd., Suite 1400, 633–6th Avenue SW, Calgary, AB T2P 2Y5, Canada.

published in the 1980s. These formulations were then applied only to one-dimensional cases in an attempt to simply show the reasonableness of the formulations. To date, the fully coupled consolidation process for multidimensional, unsaturated soil has not been solved.

This paper first presents a brief summary of the coupled formulation for the theory of consolidation of unsaturated soils and then goes on to illustrate the solution of coupled multidimensional consolidation problems. The case of the loading of a saturated sphere is first used to verify the formulation and the software implementation. An axisymmetric cylinder of soil is then used as an example problem. The initial pore-water pressure inside the soil cylinder is varied from zero to a negative value (i.e., a positive suction). The generation of the immediate pore-water pressures in response to a constant applied surface pressure is studied together with the subsequent dissipation of the excess pore-water pressures.

The results of the numerical solution of the coupled consolidation in unsaturated soils show that the Mandel–Cryer effect is minimized in the unsaturated portion of the soil. They also illustrate the primary role that the soil-water characteristic curve plays during the solution of the coupled theory of consolidation problems. In addition, the effect of full coupling of the stress and seepage problem for an unsaturated soil is demonstrated using numerical simulations of the consolidation of a soil column.

Constitutive relations and formulation of the theory of consolidation for an unsaturated soil

Biot (1941) first proposed two constitutive relationships for a consolidating soil whose water phase contained air bubbles. Although the equation was written for the case of occluded air bubbles, Fredlund and Morgenstern (1976) later showed that the constitutive equation for an unsaturated soil with a continuous air phase would have the same form. In tensorial form this constitutive relationship can be written as

$$[1] \qquad \varepsilon_{ij} = \frac{1+\nu}{E}\sigma_{ij} - \frac{\nu}{E}\sigma\delta_{ij} + \frac{u_w}{3H_1}\delta_{ij}$$

where

ε_{ij} are strain components;
σ_{ij} are stress components;
E is the elastic modulus for the solid skeleton;
ν is Poisson's ratio for the solid skeleton;
σ is the mean stress = $\sigma_{ii}/3$;
u_w is the pore-water pressure;
δ_{ij} is the Kronecker delta; and
H_1 is an additional physical constant.

The last term in this equation deals with the effect of changes in pore-water pressure which can be positive or negative. Biot (1941) correctly clarified that E and ν are "drained" soil properties. Changes in the volumetric water content, θ_w, formed a second constitutive relationship written in terms of changes in mean stress and pore-water pressure:

$$[2] \qquad \theta_w = \frac{\sigma}{H_1} + \frac{u_w}{R_1}$$

where R_1 is another physical constant relating the change in volumetric water content to a change in pore-water pressure. Equation [2] can be rewritten to include volumetric strains resulting from changes in the total stress state:

$$[3] \qquad \theta_w = \frac{K_B}{H_1}\varepsilon_v + \left(\frac{1}{R_1} - \frac{K_B}{H_1^2}\right)u_w$$

where

K_B is the bulk modulus = $E/3(1 - 2\nu)$; and
ε_v is the volumetric strain.

Equation [3] describes the change in volumetric water content caused by changes in the volumetric strain and the pore-water pressure of the soil. In summary, Biot's constitutive constants for a soil containing water with air bubbles consist of four soil properties: E, ν, H_1, and R_1. The soil properties E and ν are, respectively, the conventional elastic Young's modulus and Poisson's ratio; H_1 and R_1 are new soil properties dealing with the volumetric response of the soil and the water. Biot (1955) also gave consideration to the anisotropic case; however, this condition will not be considered in this paper.

Biot (1941) made the following assumptions in developing the above constitutive equations: (*i*) the soil is isotropic and linear elastic, (*ii*) the pore water is incompressible, (*iii*) the soil grains are incompressible, and (*iv*) small strain theory is applicable.

Dakshanamurthy et al. (1984) applied Biot's formulation to an unsaturated porous media with a continuous air phase. The constitutive equation proposed for the soil structure can be written in the following tensorial form:

$$[4] \qquad \varepsilon_{ij} = \frac{1+\nu}{E}\sigma^n_{ij} - \frac{\nu}{E}\sigma^n\delta_{ij} + \frac{u_a - u_w}{H}\delta_{ij}$$

where

σ^n_{ij} is the net stress = $\sigma_{ij} - u_a\delta_{ij}$;
σ^n is the mean net stress = $\sigma^n_{ii}/3$;
u_a is the pore-air pressure; and
H is the elastic modulus of the soil structure with respect to $(u_a - u_w)$.

By comparing eq. [4] with eq. [1], considering the special case when the pore-air pressure, u_a, is zero, and taking the sign convention used into account, it can be seen that the H modulus is related to Biot's constant H_1 through the following relationship:

$$[5] \qquad H = 3H_1$$

The constitutive equation given by Dakshanamurthy et al. (1984) for the water phase can be written as

$$[6] \qquad \theta_w = \beta\varepsilon_v + \left(\frac{1}{R} - \frac{3\beta}{H}\right)(u_a - u_w)$$

$$= \beta\varepsilon_v + \omega(u_a - u_w)$$

where

$\beta = \dfrac{3K_B}{H} = \dfrac{E}{H}\dfrac{1}{(1-2\nu)}$

$\omega = 1/R - 3\beta/H$; and
R is a modulus relating a change in volumetric water content to change in matric suction $(u_a - u_w)$.

Equation [6] is analogous to Biot's expression for volumetric water content, eq. [3]. It separates the change in volumetric water content into two components. One component is due to the volumetric strain of the soil, and the other component is due to change in matric suction. At full saturation of the soil, the change in volumetric water content is equal to the change in volumetric strain. Mathematically, the fully saturated condition is satisfied by setting $\beta = 1$ and $\omega = 0$.

A constitutive equation for the air phase was also proposed by Dakshanamurthy et al. (1984) and is given as follows:

$$[7] \qquad \theta_a = \beta\varepsilon_v + \left(\frac{1}{R'} - \frac{3\beta}{H'}\right)(u_a - u_w) = \beta\varepsilon_v + \omega'(u_a - u_w)$$

where

θ_a is the volume of air per unit volume of soil;
R' is the modulus of the air phase with respect to the matric suction $(u_a - u_w)$;
H' is the modulus of the air phase with respect to the net stress $(\sigma - u_a)$; and

$$\omega' = \frac{1}{R'} - \frac{3\beta}{H'}$$

The implementation of the constitutive equations developed by Dakshanamurthy et al. (1984) is described in the following section.

Numerical implementation of the volume–mass versus stress constitutive relations

The constitutive equations developed by Dakshanamurthy et al. (1984) were implemented into two existing finite element codes, namely SEEP/W and SIGMA/W[1], for the analysis of the coupled consolidation in unsaturated soils. The first code, SEEP/W, was developed for seepage analysis, and SIGMA/W was developed for stress-deformation analysis. The following additional simplifying assumptions were made when developing the numerical solution: (*i*) the pore-air pressure is atmospheric and remains unchanged during an analysis, and (*ii*) water flows through the soil skeleton in accordance with Darcy's Law. The first assumption limits the application of the developed code to soils for which the voids are continuous and open to the atmosphere. It simplifies the mathematical formulation by nullifying the necessity of modelling the flow of air through a soil medium. There is some indication in the literature that this assumption may not be too restrictive. Experiments carried out by Rahardjo (1990) on an unsaturated silty sand showed an essentially instantaneous dissipation of the excess pore-air pressure for the sand tested. On the other hand, the excess pore-water pressure dissipation was found to be a time-dependent process that could be simulated using the water flow partial differential equation.

To incorporate eq. [4] into the stress analysis, the strain–stress relationship for the soil structure was rewritten in an incremental form:

$$[8] \qquad \Delta\varepsilon_{ij} = \frac{1+\nu}{E}\Delta\sigma^n_{ij} - \frac{\nu}{E}\Delta\sigma^n\delta_{ij} - \frac{\Delta u_w}{H}\delta_{ij}$$

where Δ is used to denote increments.

In matrix form, the incremental stress–strain relationship for an unsaturated soil element can be written as

$$[9] \qquad \{\Delta\sigma\} = [D]\{\Delta\varepsilon\} + [D]\{m_H\}(u_w)$$

where

$[D]$ is the drained constitutive matrix; and

$$\{m_H\}^T = \left\langle \frac{1}{H}\frac{1}{H}\frac{1}{H}0 \right\rangle$$

For a soil element, which is fully saturated, the total stress in the soil structure can be given by

$$[10] \qquad \{\Delta\sigma\} = \{D\}\{\Delta\varepsilon\} + \{m\}\Delta u_w$$

where $\{m\}$ is a unit isotropic tensor, < 1 1 1 0 >. By comparing eqs. [9] and [10], the following relationship must hold when the soil is fully saturated:

$$[11] \qquad [D]\{m_H\} = \{m\}$$

The following relationship between the soil properties is satisfied for a linearly elastic and isotropic soil:

$$[12] \qquad H = \frac{E}{1-2\nu}$$

Equation [12] therefore provides a limiting value for the H modulus. By using eq. [12], the constant β in eq. [6] is evaluated to be 1.0 when the soil is fully saturated.

The constitutive relationship described by eq. [6] can also be written in the following incremental form:

$$[13] \qquad \Delta\theta_w = \beta\Delta\varepsilon_v - \omega\Delta u_w$$

At full saturation of the soil, the change in volumetric water content, $\Delta\theta_w$, is equal to the change in volumetric strain, $\Delta\varepsilon_v$. This condition is satisfied in eq. [13] by setting ω equal to zero, since β is equal to 1 when the soil is fully saturated.

The flow of pore water through an element volume of soil is given by Darcy's equation. Substituting Darcy's equation into the continuity requirement for a soil element provides an independent partial differential equation for the water phase:

$$[14] \qquad \frac{k_x}{\gamma_w}\frac{\partial^2 u_w}{\partial x^2} + \frac{k_y}{\gamma_w}\frac{\partial^2 u_w}{\partial y^2} + \frac{k_z}{\gamma_w}\frac{\partial^2 u_w}{\partial z^2} + \frac{\partial\theta_w}{\partial t} = 0$$

where

k_x, k_y, and k_z are the hydraulic conductivity or coefficient of permeability in the x, y, and z directions, respectively;
γ_w is the unit weight of water; and
t is time.

Although Darcy's law was originally developed for saturated soils, it has been demonstrated that it can also be applied to the flow of water through unsaturated soils (Richards 1931; Childs and Collis-George 1950). In addition, the coefficient of permeability can be described using mathematical func-

[1] The computer codes SEEP/W and SIGMA/W are software products developed by GEO-SLOPE International Ltd., Calgary, Alberta, Canada.

tions (Gardner 1958; van Guenuchten 1980; Fredlund et al. 1994).

Finite element formulation for coupled consolidation analysis

The equilibrium and the water-flow equations are solved simultaneously in a coupled consolidation analysis. When the two partial differential equations are uncoupled, the field variables for stress analysis in the finite element computer code are incremental displacements at the nodes. In the finite element computer code for saturated–unsaturated seepage, the field variables are hydraulic heads at the nodes.

To model the transient problem of consolidation, the incremental approach is commonly used and the system is considered to be in equilibrium during each incremental time step. In the stress analysis computer code, the piecewise finite element equilibrium equations are formulated using the principle of virtual work which states that for a system in equilibrium, the total internal virtual work is equal to the external virtual work. In the simple case when only external point loads, *F*, are applied, the virtual work equation can be written as follows:

$$[15] \quad \int \{\varepsilon^*\}^T \{\Delta\sigma\} dV = \int \{\delta^*\}^T \{\Delta F\} dV$$

where

δ^* are the virtual displacements;
ε^* are the virtual strains;
σ are the internal stresses;
V is the volume; and
the symbols Δ and { } are used to denote incremental values and a column vector, respectively.

Substituting eq. [9] into eq. [15] and applying the Galerkin procedure of weighted residuals and numerical integration, the finite element equations in the stress analysis code, satisfies the following form:

$$[16] \quad \sum [B]^T[D][B]\{\Delta\delta\} + \sum [B]^T[D]\{m_H\}\langle N\rangle\{\Delta u_w\} = \sum \Delta F$$

where

$[B]$ is the gradient matrix relating displacements to strains;
$[D]$ is the drained constitutive matrix;
N are shape functions;
$\Delta\delta$ are incremental displacements; and
Δu_w are incremental pore-water pressures.

The summation in eq. [16] is carried out for all elements. The stiffness matrix, $[K]$, and the displacement-flow coupling matrix, L_d, can be defined using the expressions shown in eqs. [17] and [18]:

$$[17] \quad [K] = [B]^T [D] [B]$$

$$[18] \quad [L_d] = [B]^T [D] \{m_H\} \langle N\rangle$$

Therefore, the equilibrium equation (eq. [16]) can be written as follows:

$$[19] \quad [K] \{\Delta\delta\} + [L_d] \{\Delta u_w\} = \{\Delta F\}$$

The summation sign has been omitted from eq. [19] for clarity. For a fully saturated soil, the coupling matrix, $[L_d]$, becomes

$$[20] \quad [L_d] = [B]^T\{m\}\langle N\rangle \quad \text{with } \{m\}^T = < 1, 1, 1, 0 >$$

Similarly, the flow equation can be formulated for a finite element analysis by first using the principle of virtual work in terms of pore-water pressure and volumetric strains. The equations are derived herein only for the two-dimensional case. If virtual pore-water pressures, u_w^*, are applied to eq. [13], the flow equation, and integration is performed over the volume of an element, the following virtual-work equation is obtained:

$$[21] \quad \int u_w^* \left[\frac{k_x}{\gamma_w} \frac{\partial u_w^*}{\partial x^2} + \frac{k_y}{\gamma_w} \frac{\partial^2 u_w}{\partial y^2} + \frac{\partial \theta_w}{\partial t} \right] dV = 0$$

Applying integration by parts to eq. [21] yields

$$[22] \quad -\int \left[\frac{k_x}{\gamma_w} \frac{\partial u_w^*}{\partial x} \frac{\partial u_w}{\partial x} + \frac{k_y}{\gamma_w} \frac{\partial u_w^*}{\partial y} \frac{\partial u_w}{\partial y} \right] dV + \int u_w^* \frac{\partial \theta_w}{\partial t} dV = \int u_w^* v_n dA$$

where v_n is the boundary flux. Substituting the expression for volumetric water content, θ_w, into eq. [6], eq. [22] becomes

$$[23] \quad -\int \left[\frac{k_x}{\gamma_w} \frac{\partial u_w^*}{\partial x} \frac{\partial u_w}{\partial x} + \frac{k_y}{\gamma_w} \frac{\partial u_w^*}{\partial y} \frac{\partial u_w}{\partial y} \right] dV + \int u_w^* \frac{\partial(\beta\varepsilon_v - \omega u_w)}{\partial t} dV = \int u_w^* v_n dA$$

Using finite element approximations, eq. [23] can be written as

$$[24] \quad -\int \frac{1}{\gamma_w} [B]^T[K_w][B]\{u_w\} dV - \int \langle N\rangle^T \langle N\rangle \left\{ \frac{\partial(\omega u_w)}{\partial t} \right\} + \int \langle N\rangle^T \{m\}^T [B] \left\{ \frac{\partial(\beta\delta)}{\partial t} \right\} dV = \int \langle N\rangle^T v_n dV$$

where

$[B]$ is the gradient matrix;
$[K_w]$ is the hydraulic conductivity (or coefficient of permeability) matrix;
$\langle N\rangle$ is the row vector of shape functions;
$\{m\}^T$ is the isotropic unit tensor, < 1 1 1 0 > ; and
δ is the nodal displacement.

In order to simplify eq. [24], the stiffness matrix, $[K_f]$, the flow-displacement coupling matrix, $[L_f]$, and the mass matrix, $[M]$, are defined using the following three equations:

$$[25] \quad [K_f] = [B]^T [K_w] [B]$$

$$[26] \quad [L_f] = \int \langle N\rangle^T \{m\}^T [B] dV$$

$$[27] \quad [M_N] = \langle N\rangle^T \langle N\rangle$$

Integrating eq. [24] from time t to time $t + \Delta t$ gives

Fig. 1. Soil-water characteristic curve for silt tailings (data from Gonzalez and Adams 1980).

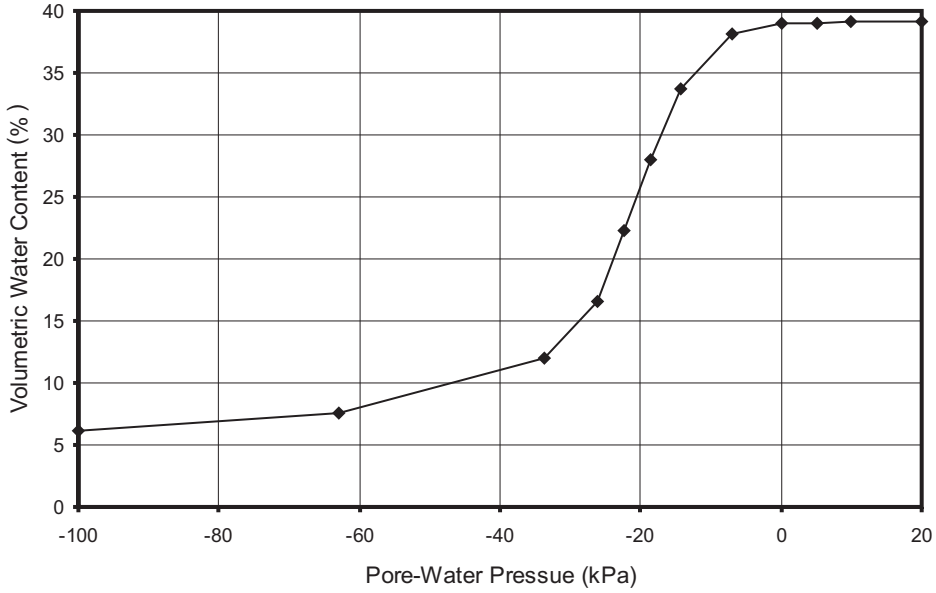

$$[28]\quad -\int_t^{t+\Delta t}\frac{1}{\gamma_w}[K_f]\{u_w\}dt-\int_t^{t+\Delta t}[M_N]\left\{\frac{\partial(\omega u_w)}{\partial t}\right\}dt + \int_t^{t+\Delta t}[L_f]\left\{\frac{\partial(\beta\delta)}{\partial t}\right\}dt=\int_t^{t+\Delta t}\langle N\rangle^T v_n dA dt$$

The following finite element equation is obtained by applying a time-differencing technique to eq. [28]:

$$[29]\quad -\frac{\Delta t}{\gamma_w}(\theta[K_f]\{u_w\}|_{t+\Delta t}+(1-\theta)[K_f]\{u_w\}|_t) -[M_N](\omega u_w)|_t^{t+\Delta t}+[L_f]\{\beta\delta\}|_t^{t+\Delta t} =\Delta t\int\langle N\rangle^T(\theta v_n|_{t+\Delta t}+(1-\theta)v_n|_t)dA$$

where θ is the time-stepping factor. If the backward (fully implicit) time-stepping scheme is used (i.e., θ equal to 1) and if the assumption is made that ω and β remain constant within a time increment, eq. [29] can be simplified as follows:

$$[30]\quad -\frac{\Delta t}{\gamma_w}[K_f]\{u_w\}|_{t+\Delta t}-\omega[M_N]\{\Delta u_w\}+\beta[L_f]\{\Delta\delta\} =\Delta t\{Q\}|_{t+\Delta t}$$

where $\{Q\}$ is the flow at boundary nodes. In order to obtain an equation that separates out the incremental pore-water pressure, the term $(\Delta t/\gamma_w)[K_f]\{u_w\}|_t$ can be added to both sides of the equation. The resultant equation describing the flow of pore water becomes

$$[31]\quad \beta[L_f]\{\Delta\delta\}-\left(\frac{\Delta t}{\gamma_w}[K_f]+\omega[M_N]\right)\{\Delta u_w\} =\Delta t\left(\{Q\}|_{t+\Delta t}+\frac{1}{\gamma_w}[K_f]\{u_w\}|_t\right)$$

In summary, the equations for coupled finite element consolidation analysis are the equilibrium equation, eq. [19], and the flow equation, eq. [31]. The equilibrium equation for saturated and unsaturated soils was formulated and assembled into the stress-analysis code together with the flow-displacement coupling matrix, $[L_f]$, of the flow equation. The flow-analysis code fills the remaining terms from the flow equation. The completed set of finite element equations is then solved within the stress-analysis code. Details of the computing procedure for this data exchange are beyond the scope of this paper.

Additional material properties for an unsaturated coupled analysis

Two additional material properties *H* and *R* are required for a fully coupled analysis involving unsaturated soils. These soil properties are not required when analyzing the saturated case. The soil parameter *H* is a modulus relating the change of volumetric strain in the soil structure to a change in suction. The soil parameter *R* is another modulus relating the change in volumetric water content to suction. Therefore, the *R* modulus is defined by the inverse of the slope of the soil-water characteristic curve. The soil-water characteristic curve can be determined in the laboratory using procedures described in Fredlund and Rahardjo (1993).

Data for a soil-water characteristic curve (SWCC) for a silt tailings are illustrated in Fig. 1 (data from Gonzalez and Adams 1980). Usually the negative pore-water pressure is written in terms of matric suction to provide a positive number. However, the pore-water pressure value has been used to show that the function is continuous into the positive pore-water pressure range. The slope of the soil-water characteristic curve increases sharply when a soil first becomes unsaturated. Correspondingly, the *R* modulus is expected to decrease significantly.

A procedure is suggested herein to obtain the *H* modulus parameter from the slope of a void ratio *e* versus matric suc-

Fig. 2. A typical void ratio vs. matric suction curve.

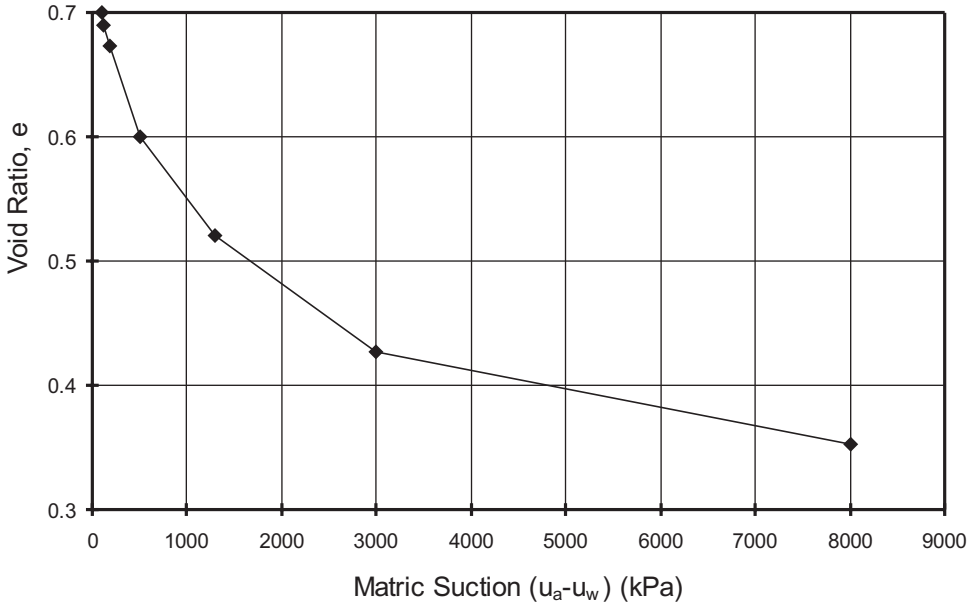

Fig. 3. A typical *H* modulus vs. matric suction curve.

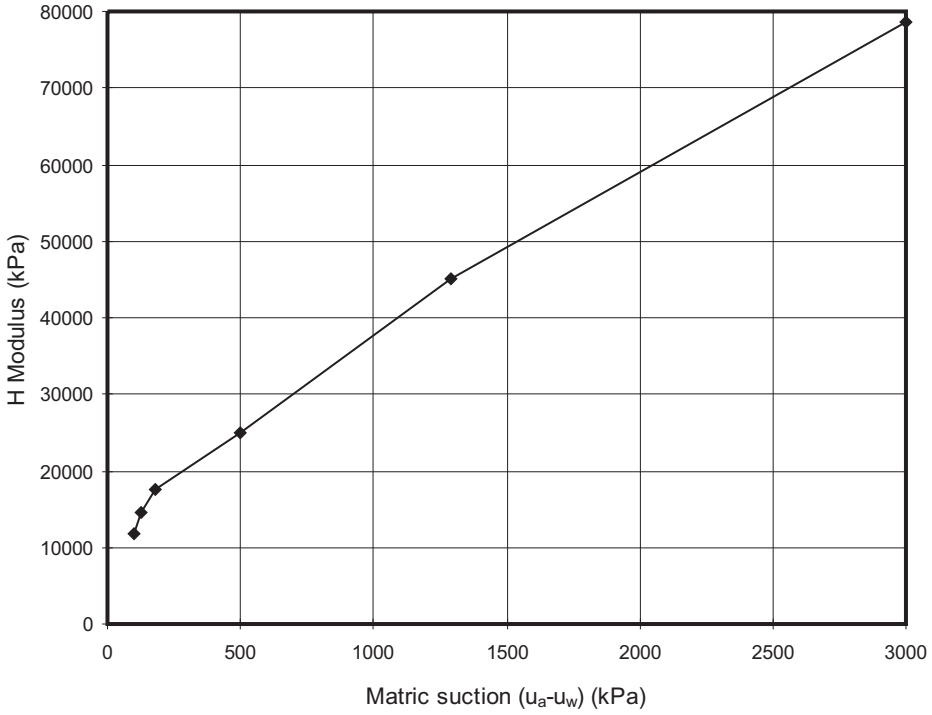

tion ($u_a - u_w$) curve. A change in the volume of a soil element can be decomposed into two parts:

[32] $$dV = dV_s + dV_v$$

where

dV_s is the change in volume of the soil particles; and
dV_v is the change in the volume of voids.

If the volume change of the soil particles, dV_s, is small and thus neglected, the volumetric strain can be approximated as follows:

[33] $$\varepsilon_v = \frac{dV}{V} \cong \frac{dV_v}{V}$$

Based on the definition of void ratio, a change in void ratio, d*e*, is given by

[34] $$de = d\left(\frac{V_v}{V_s}\right) = \frac{dV_v}{V_s} = \frac{dV_v}{(1-n)V} = \frac{d\varepsilon_v}{(1-n)}$$

where *n* is the porosity of the soil. The slope of a void ratio versus matric suction curve can be written as follows:

$$[35] \quad \frac{de}{d(u_a - u_w)} = \frac{d\varepsilon_v}{(1-n)d(u_a - u_w)}$$

When only the matric suction term of the stress state is changed in an unsaturated soil element, the incremental volumetric strain, $d\varepsilon_v$, can be written as

$$[36] \quad d\varepsilon_v = d\varepsilon_x + d\varepsilon_y + d\varepsilon_z = \frac{3d(u_a - u_w)}{H}$$

Alternatively, eq. [36] can be written as

$$[37] \quad \frac{d\varepsilon_v}{d(u_a - u_w)} = \frac{3}{H}$$

Comparing eqs. [35] and [37], the slope of a void ratio versus matric suction curve is $\{3/(1 - n)H\}$. Thus, a curve for the H modulus can be obtained for a void ratio versus matric suction curve.

Figure 2 shows a typical void ratio versus matric suction curve plotted using data presented in Fredlund and Rahardjo (1993) for a silt compacted at optimum water content. From this graph, a plot for the H modulus versus matric suction can be obtained using the procedure described above, and the results are shown in Fig. 3. A typical characteristic of the H modulus versus matric suction is that the H modulus increases significantly with increasing suction.

Example problem to verify the code and illustrate the Mandel–Cryer effect

The developed numerical computer model is first verified using Cryer's (1963) example problem involving a sphere. Then a parametric study on the effect of the R modulus on coupled consolidation is carried out using a triaxial specimen. Finally, the coupled consolidation computer code developed is applied to both saturated and unsaturated soils.

The Cryer example problem

The Cryer (1963) problem involved subjecting a sphere of saturated clay to a sudden increase in all-round confining pressure. Drainage was permitted from the surface of the sphere. Gibson et al. (1963) provided graphs of the analytical solution to this problem showing the variation of the pore-water pressure at the centre of the sphere with time for various values of Poisson's ratio.

A fully coupled consolidation analysis of Cryer's (1963) problem was conducted using the developed computer codes using the following material properties: Young's modulus, E, equal to 10 000 kPa; Poisson's ratio, ν, equal to 0.33; and a constant coefficient of permeability, k, equal to 4.91×10^{-5} m/s. In the numerical model, the clay sphere has a radius of 1 m. The sphere is subjected to a normal pressure of 100 kPa on its outside surface. The pore-water pressure at the surface of the sphere is set to zero for the analysis, indicating immediate drainage of the induced pressure. The finite element grid and the stress and displacement boundary conditions used in this analysis are shown in Fig. 4.

A comparison between the analytical and numerical results is shown in Fig. 5. The pore-water pressure, u_w, is normalized with respect to the initial applied pressure, u_0. The time factor, T, is given by the following equation:

Fig. 4. Finite element mesh and boundary conditions used for the Cryer example problem.

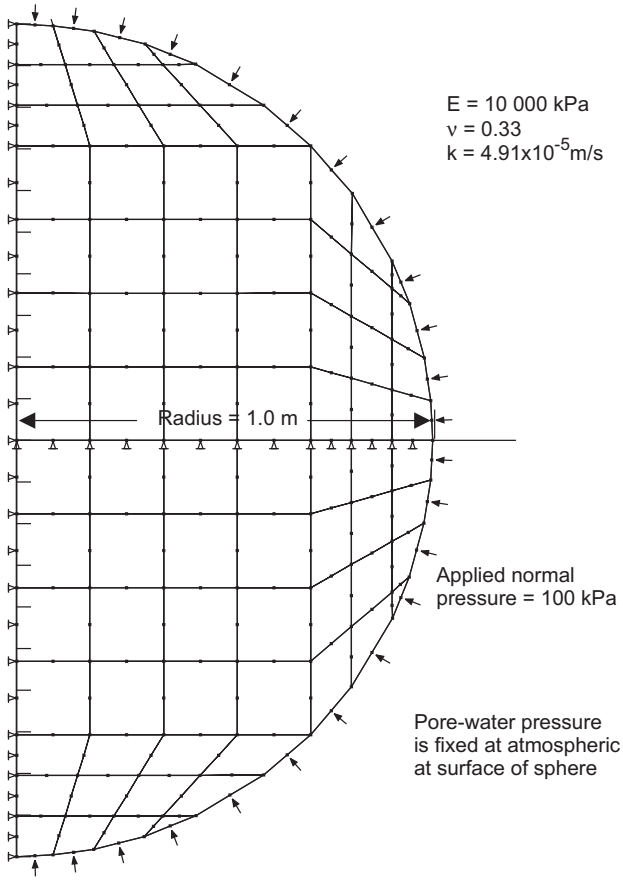

$$[38] \quad T = \frac{c_v t}{r^2} = \frac{kE(1-\nu)}{\gamma_w(1+\nu)(1-2\nu)} \frac{t}{r^2}$$

where

c_v is the coefficient of consolidation;
t is time;
r is the radius;
k is the coefficient of permeability;
E is Young's modulus;
ν is Poisson's ratio; and
γ_w is the unit weight of water.

The analytical solution and numerical solution from the developed computer code are essentially identical. The numerical solution gives a maximum peak of the nondimensionalized pore-water pressure of 1.185 as compared with 1.192 from the analytical solution. The Mandel–Cryer effect, in which the induced pore-water pressure becomes higher than the applied pressure for a saturated soil, is clearly illustrated.

Parametric study using a saturated triaxial specimen

A parametric study was also carried out using a triaxial specimen of 0.2 m radius to investigate the effect of the R modulus on coupled consolidation. The finite element mesh for the triaxial specimen is shown in Fig. 6. The material properties used are as follows: Young's modulus, E, equal to 6000 kPa; Poisson's ratio, ν, equal to 0.33; and constant co-

Fig. 5. Time variation of nondimensionalized pore-water pressure for the Cryer problem.

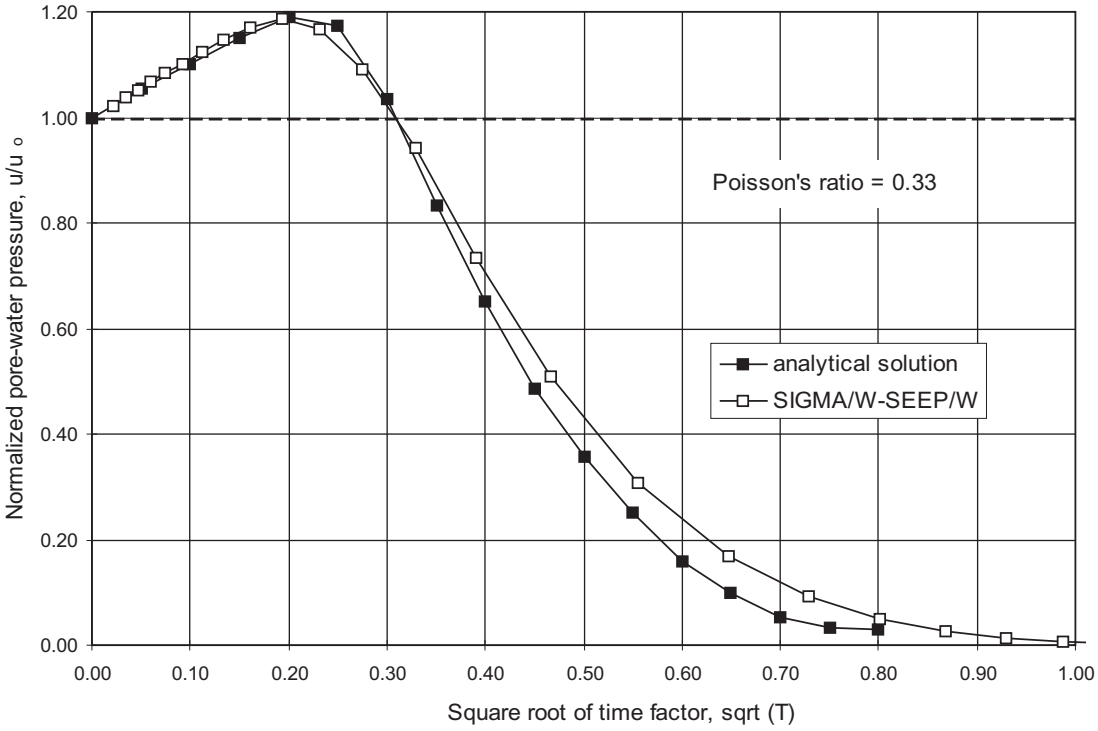

Fig. 6. Finite element mesh for Mandel's problem.

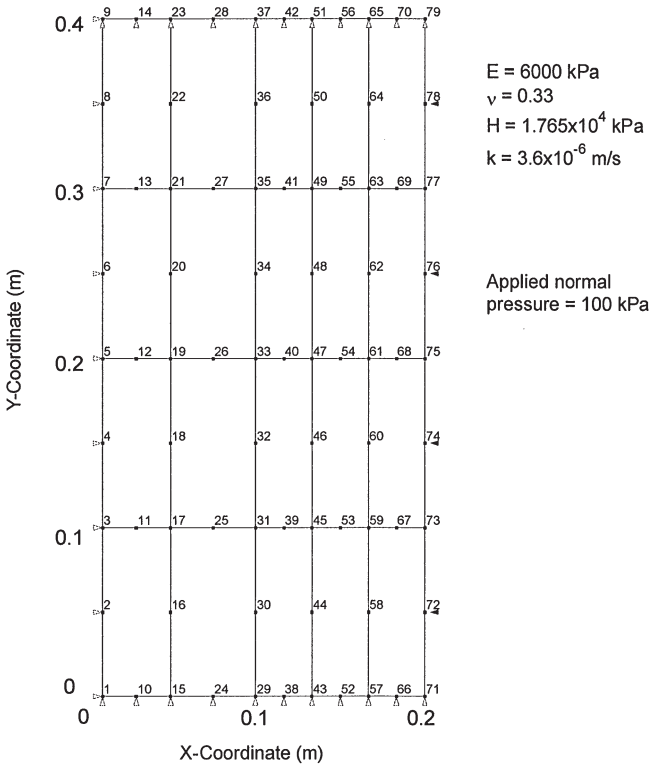

efficient of permeability, k, equal to 3.6×10^{-6} m/s. A uniform normal pressure of 100 kPa was applied to the surface of the triaxial specimen. The initial excess pore-water pressure in the sample was assumed to be zero. Since an external pressure would generate an increase in excess pore-water pressure, the parametric study was carried out under fully saturated conditions. The H modulus was assumed to be constant and given by eq. [12], corresponding to full saturation:

$$[39] \quad H = \frac{E}{(1-2\nu)} = 1.765 \times 10^4 \text{ kPa}$$

As described in the previous section, the R modulus was given by the inverse of the slope of the soil-water characteristic curve. As shown in eq. [6], the variables β and ω are used in the constitutive equation for the water phase. In order for eq. [6] to include the fully saturated case, the following conditions must be satisfied:

$$[40] \quad \beta = 1 \qquad \text{and} \qquad \omega = 0$$

At full saturation, R can be evaluated by substituting eq. [40] into eq. [12]:

$$[41] \quad \frac{1}{R} = \frac{3\beta}{H} = \frac{3(2-2\nu)}{E} = \frac{1}{K_B} = 1.700 \times 10^{-4} \text{ kPa}^{-1}$$

This represents the case where the pore water is in essence incompressible such that any external load is taken up totally by the water phase and the volumetric strain of the soil skeleton is equal to the change in volumetric water content. In the context of Skempton's pore-water pressure parameter B, this is the case of B equal to 1.0. This is designated as the reference case for the following discussion.

In this parametric study, the slope of the soil-water characteristic curve in the saturated region (i.e., pore-water pressure greater than or equal to zero) was assumed to be constant and this constant slope was varied from the reference value given by eq. [41]. Since the parametric study was carried out under fully saturated conditions, the portion of

Fig. 7. Effect of the slope of the soil-water characteristic curve on the time variation of excess pore-water pressure in a triaxial specimen. (*a*) Time duration of 14 s. (*b*) First 4 s of the analysis.

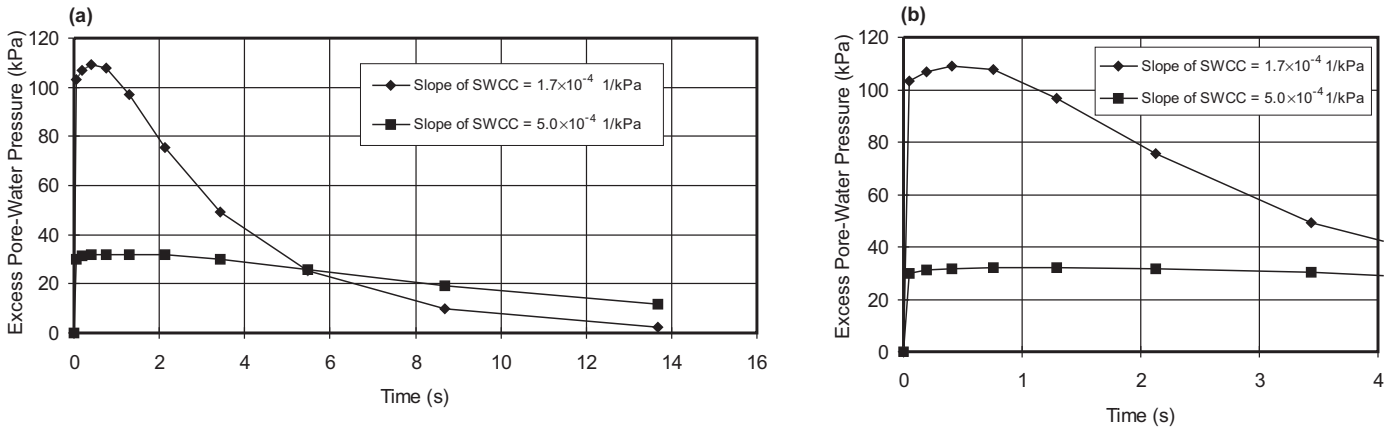

Table 1. Results of a parametric study on pore-water pressure generation in response to an applied pressure of 100 kPa.

Normalized slope	Maximum pore-water pressure (kPa)	Normalized pore-water pressure
0.49	109.18	1.09
0.59	109.18	1.09
1.00	109.18	1.09
1.06	101.62	1.02
1.18	89.30	0.89
2.94	32.09	0.32
5.88	15.51	0.16
58.82	1.51	0.02

the soil-water characteristic curve in the unsaturated region would not enter into any computations. Using the soil-water characteristic curve illustrated in Fig. 1 as an example, this parametric study would only involve the portion of the curve in the region of positive pore-water pressure (0–20 kPa), and this portion would be considered to be straight.

The reference case was first compared with a soil-water characteristic curve having a steeper slope in the positive pore-water pressure region. The slope of the curve is 5×10^{-4} kPa^{-1}, which is 2.94 times greater than 1.7×10^{-4} kPa^{-1}. Figure 7*a* compares the time variation of pore-water pressure at the centre of the triaxial specimen (i.e., at node 5) for these two soil-water characteristic curves. For the reference case, the maximum pore-water pressure generated is 109.18 kPa under an applied pressure of 100 kPa. When the pore water is slightly compressible, as represented by a steeper soil-water characteristic curve, the maximum pore-water pressure generated is 32.09 kPa under the same applied pressure. In both cases, the pore-water pressure rises with time and then dissipates as exhibited in Fig. 7*b*. In addition, the rate of pore-water pressure dissipation is much faster in the reference case. The Mandel–Cryer effect is again manifested when the soil is fully saturated.

Discussion on the effect of the slope of the soil-water characteristic curve can be simplified by normalizing the slope used in an analysis case to the slope of the reference case. A normalized slope of 1.0 would indicate the slope of the soil-water characteristic curve is equal to the reference case. A normalized slope greater than 1.0 means the slope of the soil-water characteristic curve is steeper than the reference case, or the volumetric change in soil skeleton occurs both in the water phase and the solid phase. In Table 1, the maximum pore-water pressures generated inside the soil specimen are summarized for a range of slopes for the soil-water characteristic curve. These results are presented graphically in Fig. 8. When the slope of the soil-water characteristic curve is equal to or below the limiting value given by eq. [41], the maximum pore-water pressure induced is greater than the applied pressure. In other words, the Mandel–Cryer effect is observed. These results also show that a slight reduction in the R modulus will significantly reduce the maximum pore-water pressure generated in the triaxial specimen. For the soil parameters used in this study, when R is reduced by 10%, the maximum pore-water pressure generated is only 90% of the applied pressure. Figure 8 also shows that the magnitude of the pore-water pressure response is largely controlled by the R modulus. A slight increase in the slope of the soil-water characteristic curve will suppress the Mandel–Cryer effect.

Example of coupled consolidation in an unsaturated soil

The developed computer code was also used to simulate the consolidation process in an unsaturated soil using a triaxial specimen. The geometry and the finite element mesh are the same as those used in the previously discussed parametric study. The material properties used are as follows: Young's modulus, E, equal to 6000 kPa; Poisson's ratio, ν, equal to 0.33; and a constant coefficient of permeability, k, equal to 3.6×10^{-6} m/s. A uniform normal pressure of 100 kPa was applied to the surface of the triaxial specimen. The H modulus was assumed to be constant and equal to 1.765×10^4 kPa. The soil-water characteristic curve used in solving this example is illustrated in Fig. 1.

Analyses were carried out for two initial pore-water pressure conditions at –9.81 and –19.61 kPa, respectively. Under these pore-water conditions, the triaxial specimens were initially unsaturated and under suctions of 9.81 and 19.62 kPa,

Fig. 8. Variation of the maximum excess pore-water pressure with the slope of the soil-water characteristic curve.

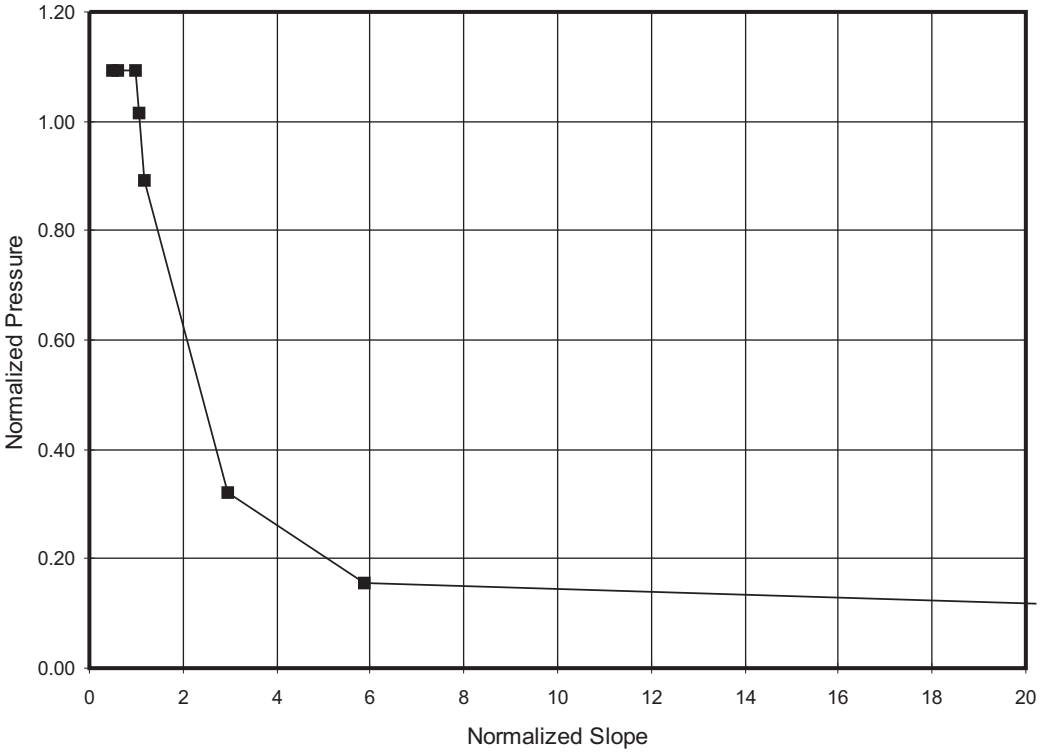

Fig. 9. Variation of example pore-water pressure with time in example problem for unsaturated soil.

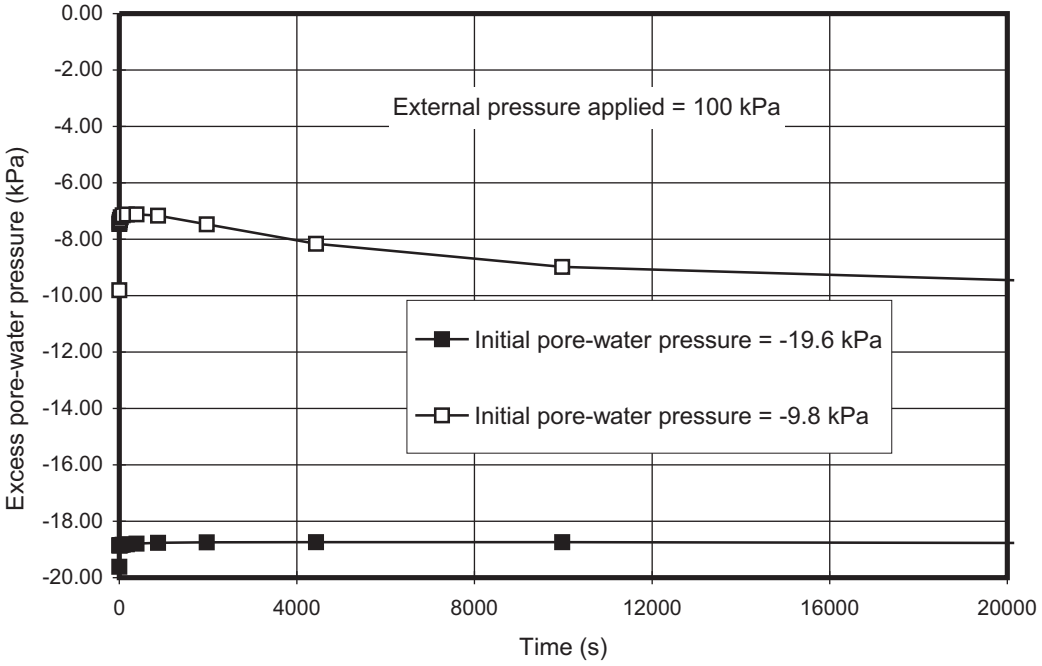

respectively. The pore-water pressure at the outside surface of the triaxial specimen was maintained at the initial value throughout the analysis.

The time variation of the excess pore-water pressure generated at the centre of the specimen (i.e., node 5) is shown in Fig. 9. In response to an externally applied pressure of 100 kPa, the maximum increases in pore-water pressure in the specimen are only 1.69 and 0.87 kPa for initial suctions of 9.81 and 19.61 kPa, respectively. This low pore-water pressure response can be attributed to the slope of the soil-water characteristic curve corresponding to the initial suctions. At a suction of 19.61 kPa, the slope of the soil-water characteristic curve is 0.00131 kPa^{-1}, and at a suction of 9.81 kPa the slope is 0.0133 kPa^{-1}. These slopes are, re-

Fig. 10. Time variation of pore-water pressure (*a*) and vertical displacement (*b*) in an unsaturated–saturated soil column.

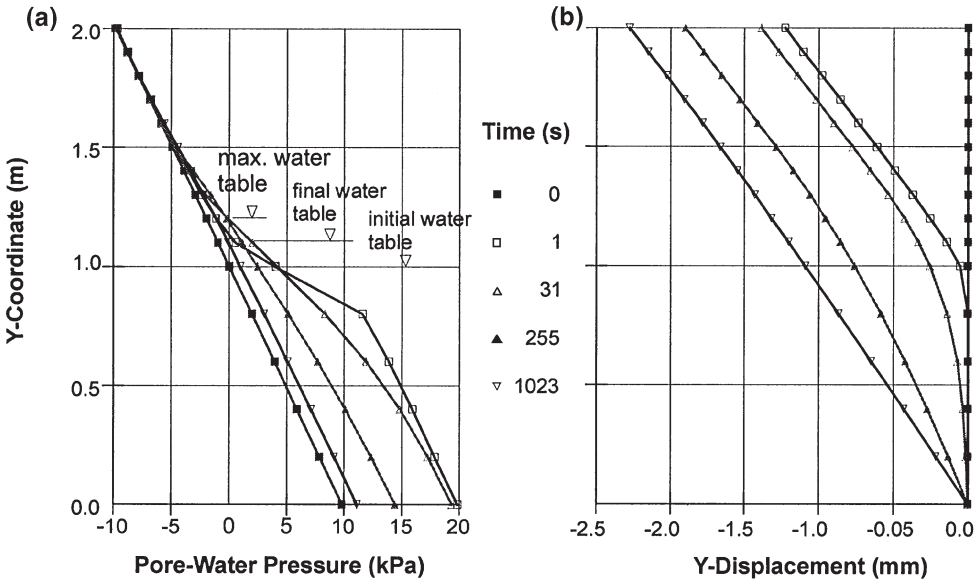

spectively, 8 and 80 times higher than that of the reference case discussed above. It should also be noted that, after the external load is applied, the induced pore-water pressure increases with time before it starts to dissipate.

Illustrative example: the consolidation of an unsaturated–saturated soil column

As mentioned in the Introduction, a common case encountered in the field is where fill is placed on the ground surface but the water table is at some depth. Figure 10 illustrates this case using a 2 m high soil column. The water table is 1 m below the surface and a load equivalent to 10 kPa is applied at the surface. The initial pore-water pressure is taken to be hydrostatic both above and below the water table. The material properties used are the same as those for the reference case of the parametric study described in the previous section.

Figure 10*a* shows the pore-water pressure distribution with depth through the soil column. After a pressure of 10 kPa is applied at the surface, the pore-water pressure increases by 10 kPa at the base of column, where the pore-water pressure is positive, whereas the pore-water pressure does not change at the top of the column, where the pore-water pressure is negative. The rate of change of pore-water response is the greatest in the middle of the sample near the initial water table.

After the load application, the pore-water pressure redistributes with time. At the bottom of the column, the pore-water pressure decreases as the soil consolidates. Above the initial water table, the pore-water pressure increases but then decreases with time. If this example is analyzed for a sufficiently long period of time, the pore-water pressure will again become completely hydrostatic, with the final water table lying slightly above the initial starting position. As shown in Fig. 10*a*, results at the last time step (time = 1023 s) are already trending towards the ultimate hydrostatic condition.

Figure 10*b* shows the displacement profiles in the soil column. Applying the 10 kPa pressure results in immediate and almost uniform incremental settlements in the unsaturated zone with little or no volume change below the initial water table. The volume-change behaviour in the saturated zone shows the typical "undrained" behaviour (minimal volume change). Then, as the soil consolidates, the soil also settles in the lower saturated zone. The rate of change of displacement with depth is almost uniform at the last time step, indicating that the consolidation is nearly complete.

Conclusions

This paper presents the numerical implementation of the coupled consolidation equations developed by Biot (1941) and Dakshanamurthy et al. (1984). Two additional parameters, *H* modulus and *R* modulus, are required for unsaturated soil. These additional parameters can be obtained from laboratory tests on unsaturated samples. The *H* modulus can be obtained from volume-change measurements in the form of a void ratio versus matric suction curve. The *R* modulus can be obtained from the slope of the soil-water characteristic curve. Although the methodology is developed using linear elastic properties for the soil, it can be extended to nonlinear material properties using a tangential modulus that remains constant during a load increment.

The developed computer code was first verified using analytical solutions for Cryer's problem for saturated soils. Results from a parametric study using a saturated soil and example problems in an unsaturated soil show that the coupled consolidation process in both saturated and unsaturated soils is controlled to a large extent by the slope of the soil-water characteristic curve (i.e., the *R* modulus). The slope of the soil-water characteristic curve controls the pore-water pressure increase in a soil specimen in response to an externally applied load. A steeper soil-water characteristic curve will give a smaller response in the pore-water pressure.

When a soil is saturated, and when the slope of the soil-water characteristic curve is equal to or below the limiting

value given by eq. [41], the Mandel–Cryer effect is induced in the soil. Under this condition, the applied pressure is taken by the water phase and can be compared to the case when the pore-water pressure parameter B is equal to 1. As the slope of the soil-water characteristic curve is increased, the portion of the external load taken up by the water phase is reduced. This latter case can be considered to be analogous to the case when the pore-water pressure parameter B is less than 1.

When an unsaturated soil is subjected to an external load, the induced pore-water pressure is much less than that when the soil is saturated. However, the manner of pore-water pressure dissipation is very similar in both saturated and unsaturated soils. After the load is applied, the induced pore-water pressure continues to increase for some time before it starts to decrease. If one considers the Mandel–Cryer effect to be such a description of pore-water pressure dissipation, it applies to both saturated and unsaturated soils.

The coupled consolidation formulation and implementation presented here for the first time makes it possible to perform a consolidation analysis of cases which have both saturated and saturated regions. Moreover, it makes it possible to analyze some swelling and shrinking due to pore-water pressure changes arising from environmental variations.

References

Biot, M.A. 1941. General theory of three-dimensional consolidation. Journal of Applied Physics, **12**(2): 155–164.

Biot, M.A. 1955. Theory of elasticity and consolidation for a porous anisotropic solid. Journal of Applied Physics, **26**(2): 182–185.

Cryer, C.W. 1963. A comparison of the three-dimensional consolidation theories of Biot and Terzaghi. Quarterly Journal of Mechanics and Applied Mathematics, **16**: 401–412.

Childs, E.C., and Collis-George, N. 1950. The permeability of porous materials. Proceedings of the Royal Society of London, Series A, **201**: 392–405.

Dakshanamurthy, V., Fredlund, D.G., and Rahardjo, H. 1984. Coupled three-dimensional consolidation theory of unsaturated porous media. *In* Proceedings of the 5th International Conference on Expansive Soils, Adelaide, Australia, pp. 99–103.

Fredlund, D.G., and Morgenstern, N.R. 1976. Constitutive relations for volume change in unsaturated soils. Canadian Geotechnical Journal, **13**: 261–276.

Fredlund, D.G., and Rahardjo, H. 1993. Soil mechanics for unsaturated soils. John Wiley & Sons, New York.

Fredlund, D.G., Xing, A., and Huang, S. 1994. Predicting the permeability function for unsaturated soils using the soil-water characteristic curve. Canadian Geotechnical Journal, **31**: 533–546.

Gardner, W.R. 1958. Some steady state solutions of the moisture flow equation with application to evaporation from a water table. Soil Science, **85**: 228–232.

Gibson, R.E., Knight, K., and Taylor, P.W. 1963. A critical experiment to examine theories of three-dimensional consolidation. *In* Proceedings of the European Conference on Soil Mechanics and Foundations, Weisbaden, Germany, Vol. 1, pp. 69–76.

Gonzalez, P.A., and Adams, B.J. 1980. Mine tailings disposal: I. Laboratory characterization of tailings. Publication 80-05, Department of Civil Engineering, University of Toronto, Toronto, Ont.

Mandel, J. 1953. Consolidation des sols (étude mathématique). Géotechnique, **3**: 287–299.

Rahardjo, H. 1990. The study of undrained and drained behaviour of saturated soils. Ph.D. dissertation, University of Saskatchewan, Saskatoon, Sask.

Richards, L.A. 1931. Capillary conduction of liquids through porous media. Physics, **1**: 318–333.

Schiffman, R.L., Chen, A.T.-F., and Jordan, J.C. 1969. An analysis of consolidation theories. Journal of the Soil Mechanics and Foundations Division, ASCE, **95**(SM1): 285–312.

van Guenuchten, M.Th. 1980. A closed-form equation of predicting the hydraulic conductivity of unsaturated soils. Soil Science Society of America Journal, **44**: 892–898.